Westerduinweg 3
1755 LE Petten
P.O. Box 15
1755 ZG Petten
The Netherlands

www.tno.nl

T +31 88 866 50 65

TNO 2022 R10384

TKI WOZ R&D EloQuENT: Wind field reconstruction from LiDAR measurements as input for aero-elastic simulation

Date 27 May 2022

Author(s) A. Pian
T. Krone
E. Rose

Copy no
No. of copies
Number of pages 22 (incl. appendices)
Number of appendices
Sponsor
Project name EloQuENT
Project number 060.34500

Summary

TNO, GE, Leosphere and ROMO wind have partnered together to investigate the effective loads quantification in enhanced and natural turbulence. The main goals of the EloQuENT project are to provide turbulent wind field for load assessment applying LiDAR wind measurements and statistical modelling instead of a point measurement at hub height and to develop a method that provides the appropriate wind field characterization for loads assessment. In this project high temporal and spatial resolution wind speed time series are generated for aero-elastic simulations. In order to achieve those, statistical means as Gaussian Processes and PyConTurb have been used on top of Lidar measurements

A measurement campaign has been carried out initially for four months, later extended to four more months, between February 2021 and September 2021 at the SIF site at Maasvlakte-Rotterdam. The data measured (LiDAR WindCube V2 Leosphere, meteorological mast, spinner anemometer and wind turbine signals) were collected in a database, quality checked and analysed. It results in a selection of 10min time series for the wind field reconstruction analysis for aeroelastic modelling.

The current report presents the methodology and the results of the application of the machine learning approach based on Gaussian Processes, for the reconstruction of a wind field covering the volume in front of the GE wind turbine Haliade X.

The methodology is divided into steps:

1 The Gaussian Processes developed in the ELFiRe project is applied to the ground base WindCube Lidar measurements time series selected in the previous WP, to produce a volume of radial wind speed at 1Hz frequency.
2 A novel statistical model is developed within this project to extract the horizontal wind speed and its components from the predicted radial wind speeds.
3 A further adaptation of the 1st results is provided for the estimation of the reconstructed wind field in specific for the aeroelastic modelling with Bladed.

The TNO machine learning methodology based on Gaussian Processes has already been validated, and it produces good estimations of the wind speed at locations close to real measurements. The uncertainty of the prediction increases with the increased distance to the real measurements data within the volume of analysis. Therefore, when applying the predicted volume of radial wind speed to the novel statistical model to extract the horizontal wind speed and its components it results in a good accuracy in the measurements along the line-of-sight. Beyond a measurement point the uncertainty of the prediction still is quite reasonable, however, there is still space to improve the predictions. Within this project an alternative solution was implemented, applying the Gaussian Process to produce a high temporal and spatial resolution wind speed profile as input for the estimation of a turbulent wind field with Pyconturb. This methodology makes use of the improvement in resolution provided by the application of the Gaussian Process while limiting its uncertainty.

Contents

1 Introduction

TNO, GE, Leosphere and ROMO Wind have partnered together to investigate the effective loads quantification in enhanced and natural turbulence. The main goals of the EloQuENT project are to provide turbulent wind field for load assessment applying LiDAR wind measurements and statistical modelling instead of a point measurement at hub height and to develop a method that provides the appropriate wind field characterization for loads assessment. In this project high temporal and spatial resolution wind speed time series are generated for aero-elastic simulations. In order to achieve those, statistical means as Gaussian Processes and PyConTurb [1]have been used on top of Lidar measurements

This new method will be developed using an existing data set comprising met mast signals, LiDAR and wind turbine's data from a large wind turbine in complex wind flow conditions, in order to enhanced lidar wind field reconstruction.

For this purpose a four month measurements campaign, later extended to eight months, has been realized at the SIF site at Maasvlakte-Rotterdam. The data measured were collected in a common database which includes the following sources: Leosphere WindCube V2 LiDAR , Met mast, Spinner Anemometer and wind turbine data. The data containing wind velocity, statistics, and other parameters such as pressure, temperature, loads were quality checked and analysed and times series fulfilling aeroelastic modelling requirements were selected in the previous work package [2], the data measurements from the Spinner anemometer will not be used in the analysis presented in this report.

This report presents the estimation of a reconstructed wind field for horizontal velocity applying the Gaussian Processes (GPs) to LiDAR measurements. First a statistical model was developed to translate predicted radial wind speed produced by the GPs into horizonal wind speed and its component. Then a further methodology is provided to produce a wind field where the GPs is applied to the estimation of a high resolution wind speed profile, input for the model Pyconturb. The output represents the wind field needed for the aeroelastic modelling.

The structure of the report is as follows:
Chapter 2 describes the step 1 of the analysis for the wind field reconstruction: the Gaussian Process is applied to the selected time series to produce a volume of radial wind speed for three test resolutions.
Chapter 3 provides the step 2 of the analysis: the methodology developed in this project to transform the predicted radial wind speed into horizontal wind speed through a statistical model.
Chapter 4 offers the adaptation of the output from the 1st step analysis for the turbulent model Pyconturb for the aeroelastic modelling analysis.
Conclusions are presented in Chapter 5.

2 Step 1: Gaussian Processes

This chapter presents the first step in the reconstruction of the wind field. In specific, the results from the previous work package: selected time series of LiDAR measurements, are applied to the Gaussian Process to estimate predicted radial wind speed covering a volume of space in front of the rotor area.

2.1 WP1 conclusion summary

In WP1 a database was created with the following measurements:

- Leosphere WindCube V2 LiDAR
- Met mast
- Turbine data
- Spinner anemometer (the data measurements from the Spinner anemometer will not be used in the analysis presented in this report).

The measurement campaign ran from February 2021 till the end of September 2021, although the turbine was operating for a very limited time and the summer months were characterized with lower wind speeds.

The dataset was analysed and quality checked. From the measurements, time series of 600 seconds length were selected for the aeroelastic modelling. The selection of the time series was made on the following parameters constraints:

1 LiDAR signal availability 100% at 135m;
2 Wind direction from the selected wind sector: 250° to 300°;
3 Met mast signals 100% availability;
4 Wind turbine operational at normal condition: active power;
5 Average wind speed for the selected 10 minutes of 8m/s, 10m/s and 12m/s with a wind speed bin of 1m/s.

A total of 6 time series for each average wind speed were selected, for a total of 18 samples.

An additional analysis was applied to the September measurements, the only period where all the instrumentation were operating (LiDAR, met mast and Spinner anemometer) and in which the wind speeds were particularly lower than the winter months. To identify 10 minutes periods during this month, the average wind speed was lowered to 7m/s with a wind speed bin of 1m/s to select 4 time series.

2.2 The method: Gaussian Process

A machine learning method based on Gaussian Process (GP) regression was previously developed in the ELFiRe project to improve the wind field reconstruction from LiDAR measurements. GP is a novel approach for this application and its validations are presented in several studies [3], [4], [5], [6]. Within this project, the method programmed in MATLAB® has been converted into Python.

The volume of predicted radial wind speed is selected in the area above the LiDAR covering the rotor area of the GE Haliade X 13 MW wind turbine, located in the vicinity of the LiDAR and meteorological mast at the Maasvlakte 2, Rotterdam, The Netherlands. The GE Haliade X 13MW is a direct drive wind turbine with variable

speed, active pitch control, a rated power of 13 MW, hub height of 135 m and a rotor diameter of 220 m. The volume selected for this project is adjusted to the rotor diameter, in particular based on the settings of Bladed [7], the aeroelastic modelling simulation tool used by GE, with the height of the turbulent wind field centred at the hub height. The total area simulated by Bladed covers a volume of 240m (width) and 270m (height) for a total of 48 x 48 x 39 grid points.

In order to assess the use of the GP with the dataset, a test of the resolution was performed. A coarse horizontal grid, spanning 200m both North and East, was generated at each of the nine measurement heights of the LiDAR: 40, 60, 80, 107, 130, 135, 162, 190, and 217 meters. An additional plane of predictions was also made at 240m. This cube of predictions was made at 1 second intervals over the course of each entire 600 second measurement period. For illustrating results, a reference time period of the 14th of March,17:00 UTC was chosen, and it is referred to as the reference period from here on out. In this period the LiDAR measures at 135m a 10-min average wind speed of 7.6 m/s, a 10-min average wind direction of 269.5° and a standard deviation of 0.78 m/s.

Due to the high computational load, 10 seconds time series for a lower grid resolutions were tested first. The resolution of the grid at each height was varied between three testing sizes: 7x7, 11x11, and 21x21 grid points. This was done to find an optimum: more grid points leads to a more detailed view of the incoming wind, but takes longer to process within the methods. Vertical resolution was kept the same, predicting at the 10 measured heights of the lidar.

A parameter-smoothing GP layer was not applied, because the length of the time series was considered short enough to be able to be represented well by a single GP. As such, each 10-minute time series had its own GP fit to the unique data, from which predictions were made.

The wind velocity reconstruction requires a volume of predictions at different locations, and as such the x, y, and z positions of each measurement relative to the LiDAR were calculated. This was done by looking at the internal LiDAR coordinate system, where each beam corresponds to a cardinal direction (0°, 90°, 180°, or 270° degrees). The coordinate system used for this project can be seen in Figure 2.1. Finally, a 30° offset was recorded in the LiDAR installation, which was accounted for.

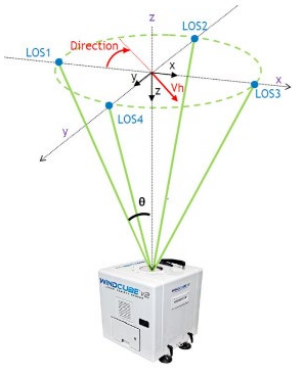

Figure 2.1 LiDAR coordinate system, as described in [8]

2.3 Results

The results of the resolution testing can be seen in Figure 2.2, Figure 2.3 and Figure 2.4 below, which show the radial wind speeds predicted within the volumes for a single timestamp. All three cubes were able to be run within a reasonable time frame to generate the GP solution, with all simulations running within one hour, and produce values which are expected. As such, since high-resolution cubes could be ran without significant delay, the 21x21 cubes were used for further analysis.

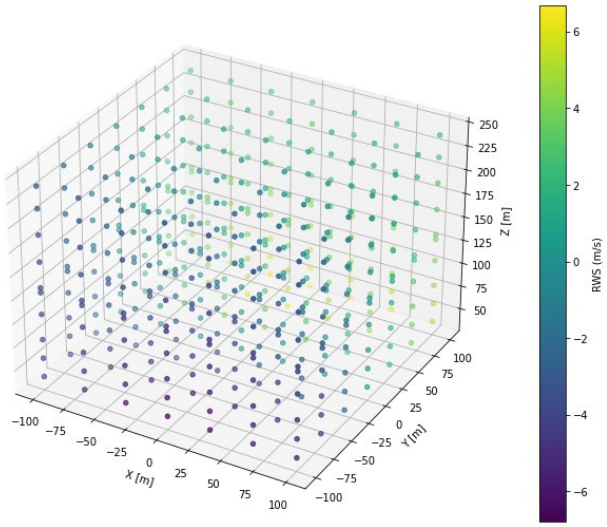

Figure 2.2 Radial wind speeds for a 7x7 grid of prediction points

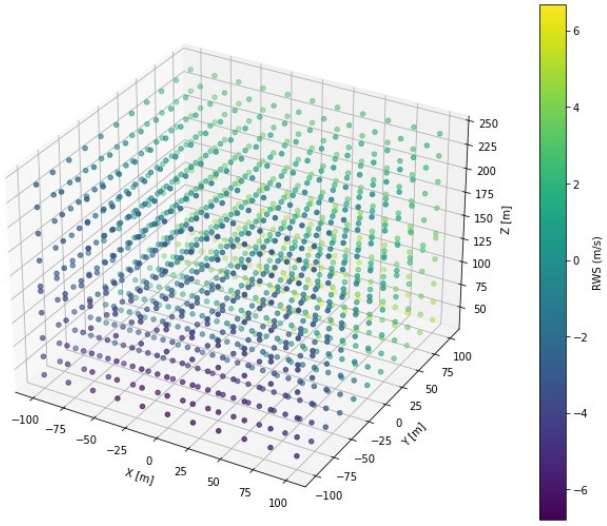

Figure 2.3 Radial wind speeds for a 11x11 grid of prediction points

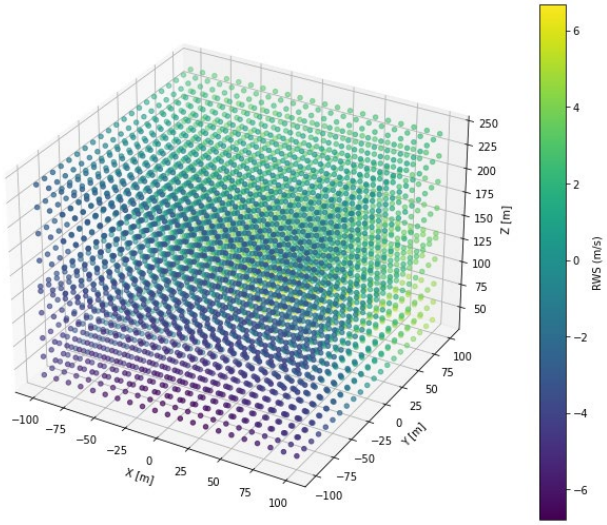

Figure 2.4 Radial wind speeds for a 21x21 grid of prediction points

It is important to note the accuracy of the predictions. The GP method outputs an estimate of the uncertainty: the prediction standard deviation. In order to show how this looks for this configuration, Figure 2.5 below contains a very dense grid at a single timestamp, both for all heights and a reference height, and coloured by the prediction standard deviation. At the line-of-sight (LOS) prediction locations this uncertainty drops, as the method has data about what is occurring at those points. However, it can be seen that the standard deviation reaches a maximum constant value elsewhere. This tends to translate to the prediction at that point reaching a constant, average value. This is especially true outside of the boundaries of the LiDAR measurement volume; here, with no information about what is occurring, the GP tends towards the average value of the LOS speed over all heights and time steps. The consequences of this will be seen in the next section. Note that the prediction uncertainty seen stands for the GP as a whole, and does not change as a function of the resolution. As such, the 7x7, 11x11, and 21x21 resolution predictions all have the level of prediction uncertainty shown in Figure 2.5.

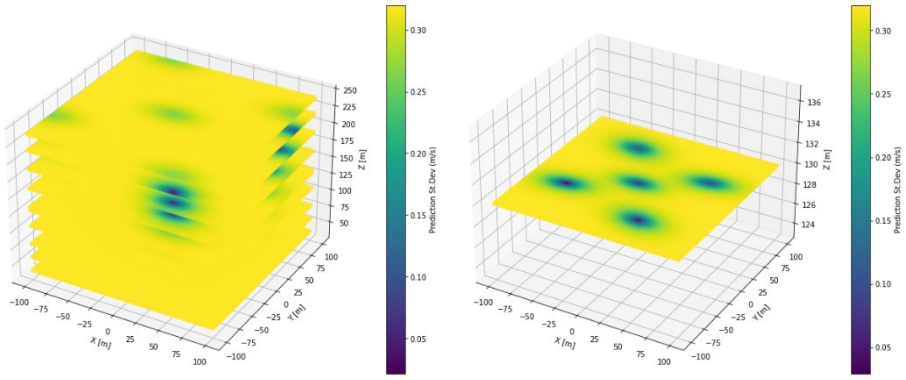

Figure 2.5 Prediction standard deviation for a high-resolution grid at every height (left) and at the reference height (right)

3 Step 2: Wind Velocity Reconstruction

Once the volume of predicted radial wind speed has been produced (Step 1), a statistical model is applied to obtain the horizontal and vertical components of the wind speed. The statistical model is first described and then the project case results are presented.

3.1 Statistical modelling methodology

As mentioned in the previous section, the LiDAR system from Leosphere uses a standard spherical co-ordinate system. The beam measures at selected distances a component of the wind velocity vector. To create measures for the horizontal windspeed and the wind direction, we reconstruct the three directions of the wind measured by the LiDAR and provided as radial wind speed: *vx, vy* and *vz*. The wind speed measured by the LiDAR beam is calculated as the following equation according to the spherical co-ordinates:

$$v_{rad} = \sin\phi \sin\theta \times v_x + \cos\phi \sin\theta \times v_y + \cos\theta\, v_z \quad (1)$$

Where v_{rad} is the radial windspeed as predicted by the GP or measured by the LiDAR, θ is the zenith as calculated by:

$$zenith = \arctan\frac{\sqrt{X^2 + Y^2}}{Z}$$

And ϕ is the azimuth as calculated by:

$$azimuth = \arctan\frac{Y}{X}$$

Where X is the distance from the middle on the southern to northern axis, and Y is the distance from the middle on the western to eastern axis, see **Fout!**

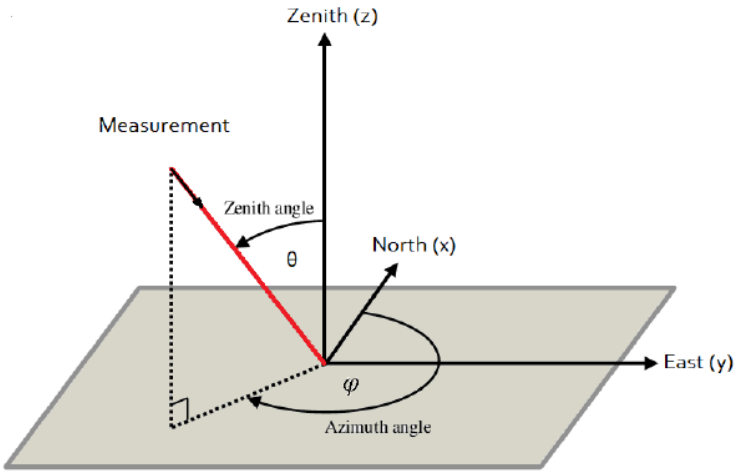

Figure 3.1 Spherical co-ordinate system for Lidar beam measurements

Verwijzingsbron niet gevonden..

The estimation of a wind field is problematic when we take into account all three wind speed vector components; the model is quickly unidentified, and the formula cannot be resolved using a closed-form equation. As such, a two-step method using Bayesian Analysis is used.

In the first step, the average wind field per second and per height level (Z) is estimated. In this step, the Bayesian program Rstan [9], run with RStudio, is used to estimate the wind field using the v_{rad} formula in which we assume $v_x, v_y \; and \; v_z$ are each uniform in each the horizontal plane, i.e., the only difference allowed is for different heights and different timepoints, giving us:

$$vrad_{\,x,y,z,t} = \sin\phi \sin\theta \times v_{x_{z,t}} + \cos\phi \sin\theta \times v_{y_{z,t}} + \cos\theta \, v_{z_{z,t}} + \varepsilon,$$

$$\varepsilon \sim Normal(0, \sigma_\varepsilon)$$

where *Normal* stands for normal distribution with 0 mean and standard deviation of the estimated error. This allows us to estimate the average windspeed on $v_x, v_y \; and \; v_z$ per time point *t* and per height *z*. The priors used for this model are:

$$vx_{z,t} \sim Normal\ (0{,}10)$$
$$vy_{z,t} \sim Normal\ (0{,}10)$$
$$vz_{z,t} \sim Normal\ (0{,}10)$$
$$\sigma_\varepsilon \sim Normal\ (0.3{,}0.1)$$

In the second step, we use this information as a prior to estimate a heterogenous wind field. For each point as estimated by the LiDAR we estimate the $v_x, v_y \; and \; v_z$ and the estimated error w using formula (1):

$$vrad_{\,x,y,z,t} = \sin\phi \sin\theta \times vx_{x,y,z,t} + \cos\phi \sin\theta \times vy_{x,y,z,t} + \cos\theta \, vz_{x,y,z,t} + w,$$

$$w \sim Normal(0, \sigma_w)$$

Here, the priors used are based on the first estimation:

$$vx_{x,y,z,t} \sim Normal\ (vx_{z,t}, \sigma_\varepsilon)$$
$$vy_{z,t} \sim Normal\ (vy_{z,t}, \sigma_\varepsilon)$$
$$vz_{z,t} \sim Normal\ (vz_{z,t}, \sigma_\varepsilon)$$

Furthermore, we add a correlational dependency on three points for each of $v_x, v_y \; and \; v_z$ to allow for a faster and more reliable estimation:

$$vx_{x,y,z,t} = \beta_1 vx_{x-1,y,z,t} + \beta_2 vx_{x,y-1,z,t} + \beta_3 vx_{x-1,y-1,z,t} + \epsilon, \qquad \epsilon \sim N(0, \sigma_\epsilon)$$
$$vy_{x,y,z,t} = \beta_1 vy_{x-1,y,z,t} + \beta_2 vy_{x,y-1,z,t} + \beta_3 vy_{x-1,y-1,z,t} + \epsilon, \qquad \epsilon \sim N(0, \sigma_\epsilon)$$
$$vz_{x,y,z,t} = \beta_1 vz_{x-1,y,z,t} + \beta_2 vz_{x,y-1,z,t} + \beta_3 vz_{x-1,y-1,z,t} + \epsilon, \qquad \epsilon \sim N(0, \sigma_\epsilon)$$

Where vx, vy, vz are the windspeeds components, β_1, β_2, and β_3 the correlation coefficients between the estimated data point and nearby datapoints and ϵ the estimation error. The priors for the beta are Normal (0.33, 0.1), to account for the fact that the three nearby cells combined are assumed to be a close estimation of the estimated cell. The definition of the correlation between data points combined with

the prior homogenous wind field as created in step 1 allows us to identify the model and thus estimate an vx, vy, vz out of v_{rad} for each data point.
Using the estimated horizontal components of windspeed, we can then estimate the total horizontal windspeed and direction:

$$Windspeed = \sqrt{vx^2 + vy^2}$$

$$Wind\ direction = \arctan \frac{vx}{vy}$$

3.2 The results

The three testing time series of a volume of radial wind speed predicted by the GP in the step 1 are here applied in the statistical model to obtain horizontal wind speed for the same volume. In specific, horizontal wind speed on the x-axes at 130m height for the three testing resolution are shown in Figure 3.2, the wind speed components, v_x, v_y and horizontal wind speed at 130m height for the 21x21 resolution in Figure 3.3, the horizontal wind speed at each height for the 21x21 resolution are provided in Figure 3.4 and finally, horizontal wind speed at 130m for 10 sec at 21x21 resolution in Figure 3.5. From the figures it is visible an inhomogeneities in the horizontal wind field which occur at the relative position of the lidar beams.

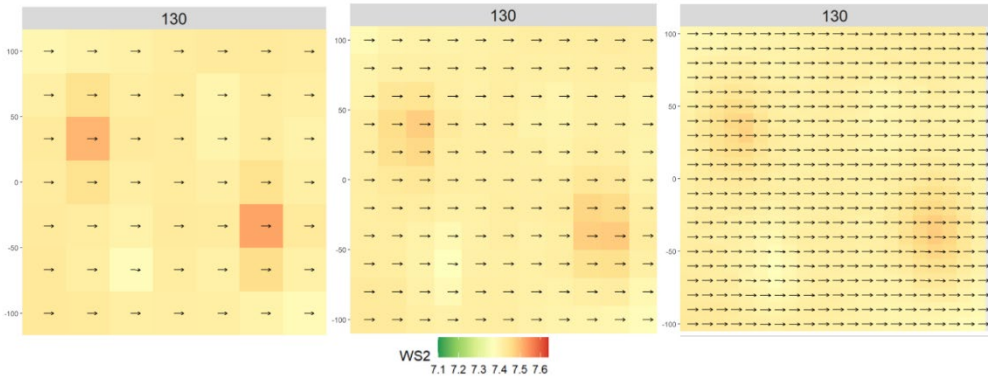

Figure 3.2 Horizontal wind speed at 130m height for 1 sec for each grid size resolution (7x7, 11x11 and 21x21)

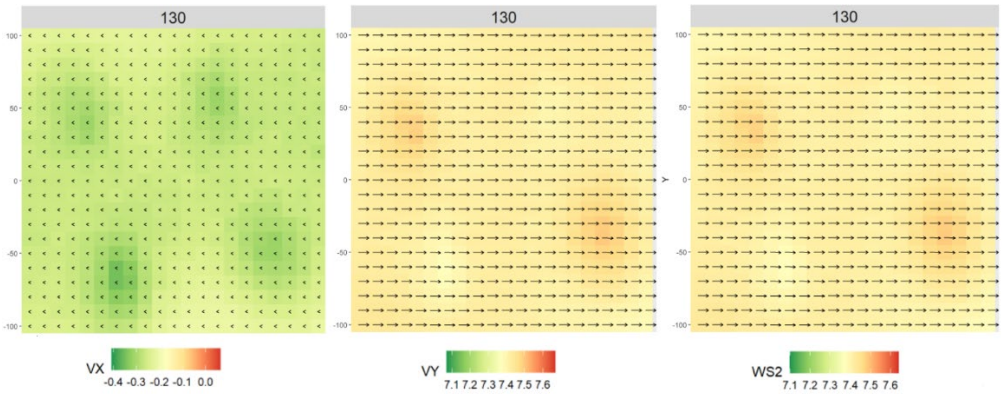

Figure 3.3 Wind speed component at 130m, grid size 21x21, left: v_x, centre: v_y, right horizontal wind speed

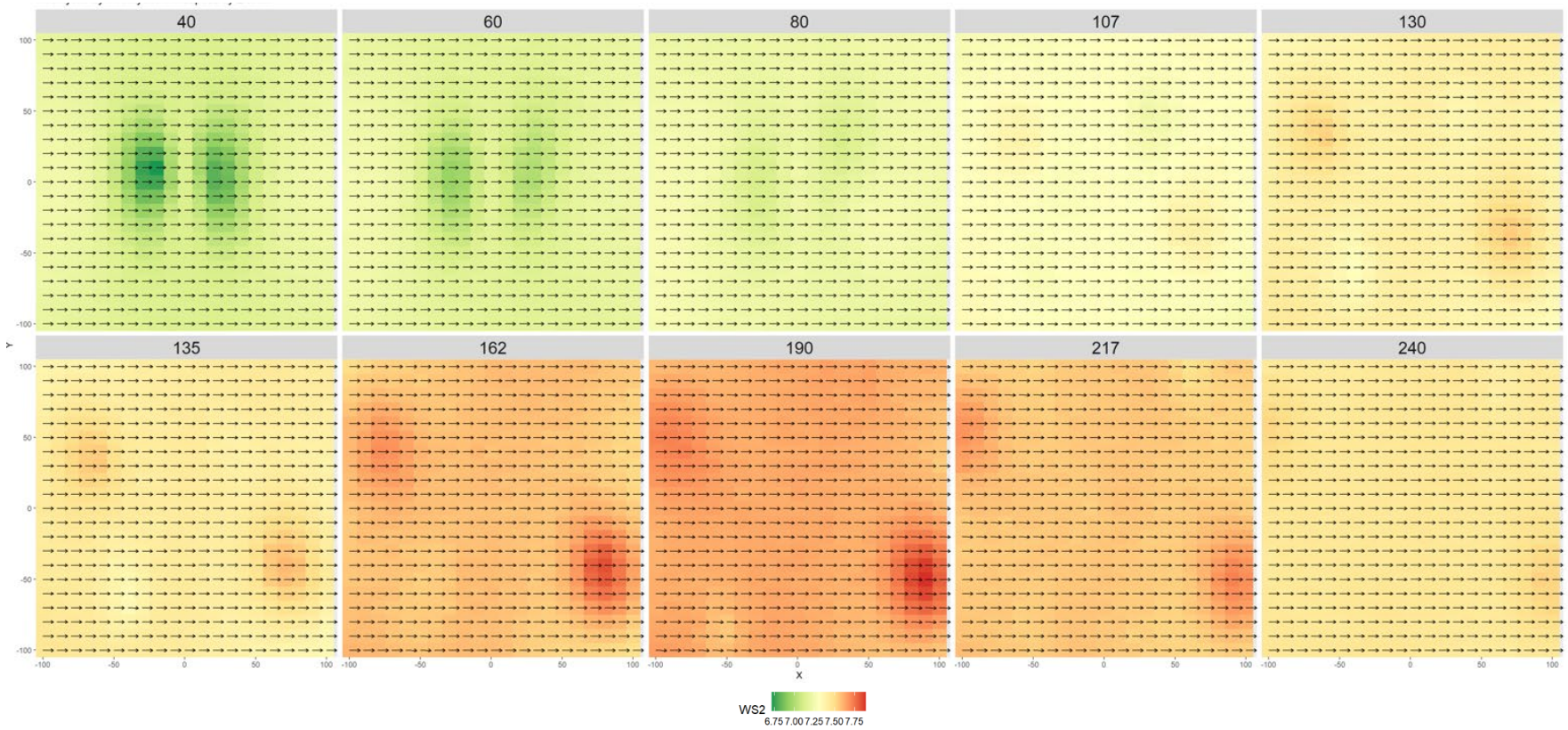

Figure 3.4 Horizontal wind speed, grid size 21x21, 1sec, all heights 40, 60, 80, 107, 130, 135, 162, 190, 217, 240m

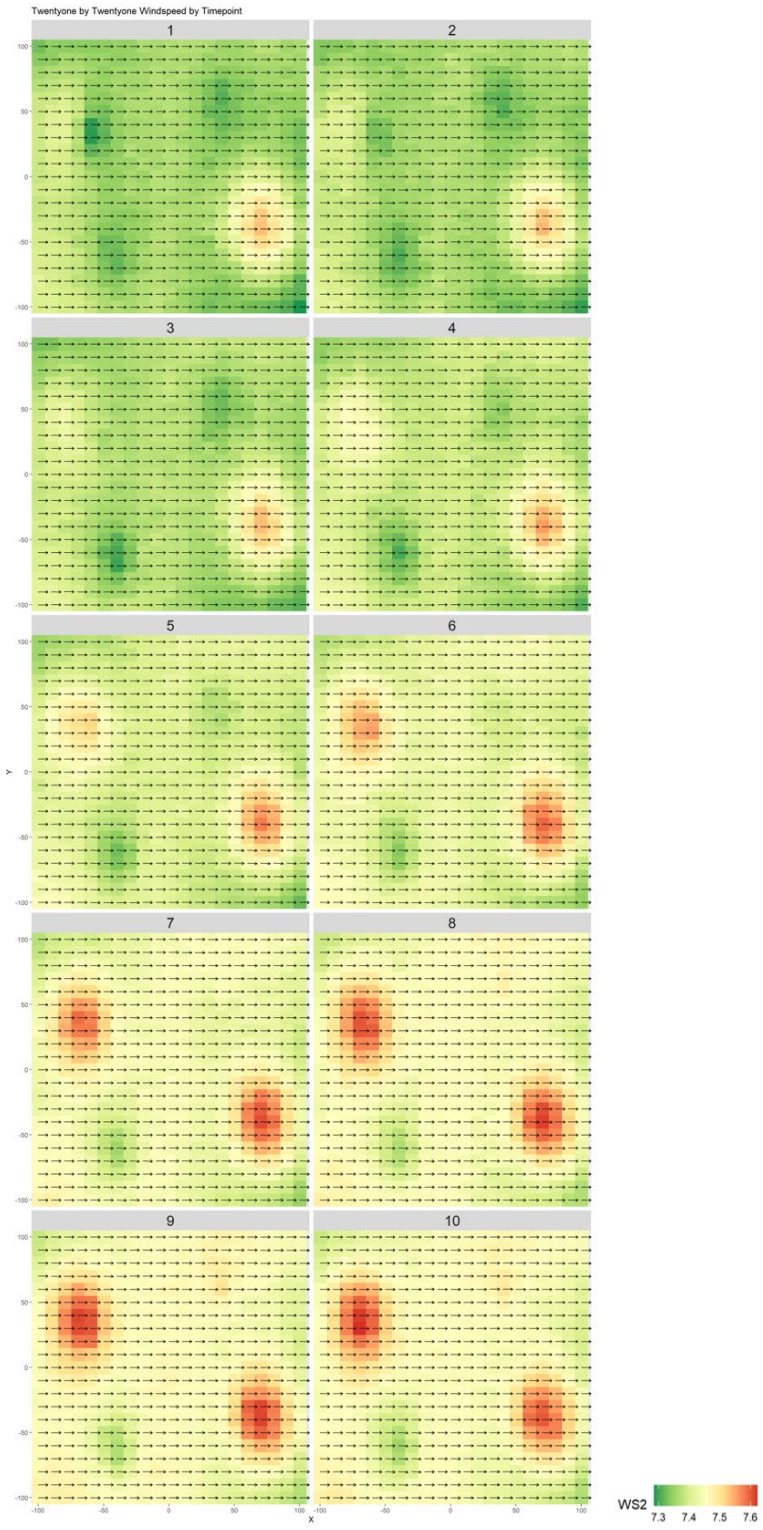

Figure 3.5 Wind speeds at 135 per 10 secs at 21x21 resolution

From the above illustrations, it was concluded that the statistical model is working well to generate horizontal wind speeds at measurements points. Nevertheless, beyond a measurement point the uncertainty of the prediction still is quite reasonable.

4 Input for aeroelastic modelling

For aeroelastic modelling, the end goal of this project, it has been decided to provide a further wind field estimation time series. This is presented in the following section.

4.1 Methodology

To reconstruct the wind fields while utilizing the GP's is to instead predict at very high resolution along the beams. Predictions were made along each of the five LiDAR lines of sight (LOS's). At every second, a plane of five predictions was made at every 1 meter height, from 40m to 217m. This provides updated LiDAR measurements at all locations every second (where the LiDAR regularly updates a single beam's measurements every five seconds), for a much higher resolution of heights. This methodology allows for a homogenous reconstruction at every predicted height and timestamp, transforming the ground-based LiDAR into a high-resolution meteorological mast. Figure 4.1 shows this configuration of predictions.

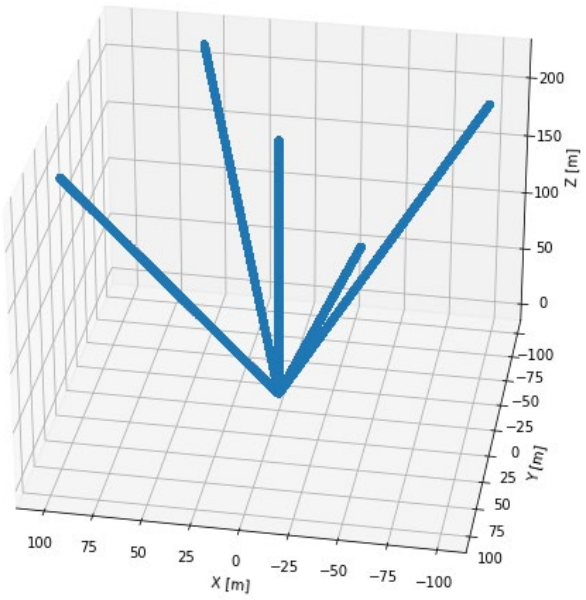

Figure 4.1 Gaussian process prediction locations along the LOS's of the ground-based LiDAR

With this prediction pattern, a homogenous reconstruction following the equations below, could be completed, where RWS is the radial wind speed measurement from the GP in m/s, and θ is the zenith angle utilized above in radians.

$$V_x^* = \frac{RWS_1 - RWS_3}{2\sin\theta}$$
$$V_y^* = \frac{RWS_2 - RWS_4}{2\sin\theta}$$
$$V_z = RWS_5$$

These provide the wind speeds along the North/South and East/West orientations of the LiDAR (V_x^* and V_y^*). However, this reconstruction assumes that the RWS's are perfectly aligned with the cardinal directions and do not take into account the physical LiDAR offset of 30° included earlier. This is corrected for in the following equations, ending with a longitudinal, lateral, and vertical wind speed (V_x, V_y, and V_z respectively) at every height for the given time series and a given offset, φ_o.

$$V_x = V_x^* \cos\varphi_o - V_y^* \sin\varphi_o$$
$$V_y = V_x^* \sin\varphi_o + V_y^* \cos\varphi_o$$

With the horizontal wind reconstructed in in front of the turbine, Pyconturb can be used to propagate the wind further. Pyconturb, as outlined in [10], is an open-source turbulence box generator developed by DTU. It was used for this exact purpose: to generate a turbulence box utilizing the LiDAR and GP reconstructions to constrain the output.

However, Pyconturb uses a different coordinate system, with wind inflow towards the turbine considered positive V_x, V_y the lateral flow going left if facing the same direction as the inflow, and $\underline{V_z}$ positive upwards. The exact yaw direction of the turbine at each period of time is unknown. As such, in order to translate the wind into this coordinate system, the average wind direction was taken at hub height for each time period. Then, every data point is translated assuming that positive V_x flows in this direction, using the following equations, where $\Delta\varphi$ is the difference at each time between the actual and average inflow directions, V_{Hor} is the horizontal wind speed in the LiDAR coordinate frame, and $V_{x,P}$, $V_{y,P}$, and $V_{z,P}$ are the velocity components in the Pyconturb reference frame.

$$V_{Hor} = \sqrt{V_x^2 + V_y^2}$$
$$V_{x,P} = V_{Hor} \cos\Delta\varphi$$
$$V_{y,P} = V_{Hor} \sin\Delta\varphi$$
$$V_{z,P} = -V_z$$

As stated previously, the required grid for simulations is 48x39 points spanning 240m laterally and 270m vertically. 600 seconds of data were simulated using Pyconturb with this grid, shown in Figure 4.2, which also shows the location of the LiDAR/GP predictions. Pyconturb was ran using a power law fit for the wind speeds, and following the actual wind standard deviations from the high resolution profile. Three parameter inputs were required for the simulations: reference height, reference wind speed, and the power law shear exponent, see Table 1. Additionally, the entire high resolution wind speed time series is also input, from which Pyconturb works with the standard deviation. The shear exponent was obtained by fitting the LiDAR wind speed high resolution predictions to a logarithmic function, a standard least-square fitting, between the nine LiDAR prediction heights. Reference height was taken to be turbine hub height, and the reference wind speed is the average wind speed in the 10 minutes at hub height. For the same 10-minute reference period as above, 14th of March,17:00 UTC, these values are listed below in

Table 1.

Table 1 Pyconturb input parameters for the reference time period

Parameter	Value
Reference Height	135m
Reference Wind Speed	7.6 m/s
Shear Exponent	0.36

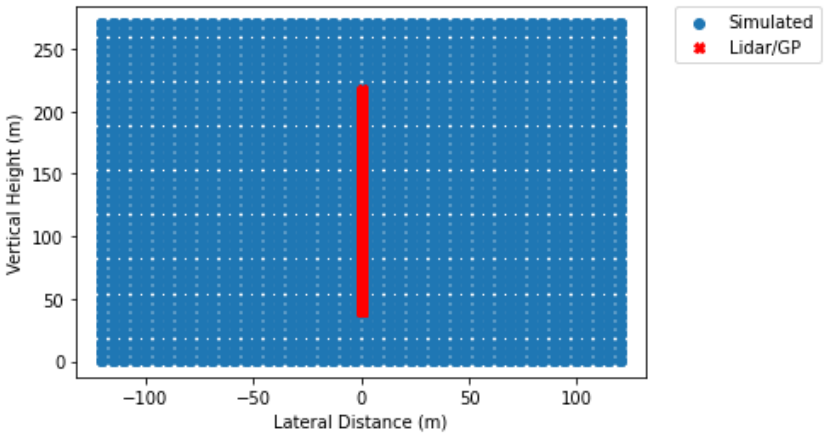

Figure 4.2 Locations of the simulated, as well as constraining, points in the Pyconturb turbulence box generation

4.2 Results

Figure 4.3 below shows the turbulence box generated by Pyconturb for one timestamp, for a random seed. The vertical and lateral wind speeds are all relatively low, and average around zero as expected. The longitudinal wind speed, representing the turbine inflow, increases with height, and when viewed over time turbulent pockets of varying length-scales can be seen.

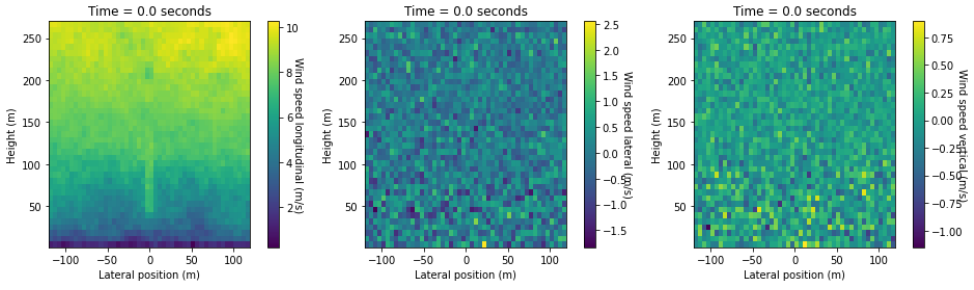

Figure 4.3 Longitudinal (left), lateral (centre) and vertical (right) turbulent outputs from Pyconturb for the reference time period

In order to check the validity of the generated turbulence box, and to ensure the LiDAR/GP constraints were being followed, a number of checks were completed. Figure 4.4 shows the average and standard deviation of the longitudinal component of the turbulence box as a function of height, comparing the mean to that of the LiDAR/GP constraints. It can be seen that the Pyconturb profile matches the shearing behaviour from the constraint dataset, and follows the overall turbulence of the data as well.

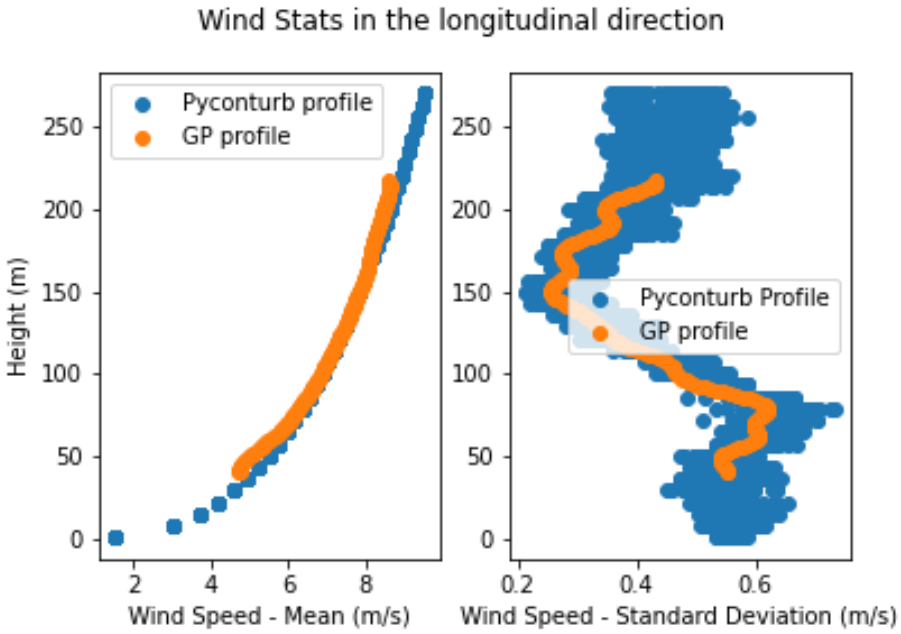

Figure 4.4 Wind speed average (left) and standard deviation (right) for the Pyconturb longitudinal wind speed profile at the reference time. Mean values are included for the LiDAR/GP averages, for comparison

Figure 4.5, Figure 4.6, and Figure 4.7 show the longitudinal wind profiles at three points close to the LiDAR measurement locations: 40m, 135m, and 217m. At hub height, the average wind speed, turbulence, and overall behaviour of the wind is consistent between the measured values and those simulated from Pyconturb. At 40m and 217m, there are slight differences in mean wind speed, but the turbulence is consistent.

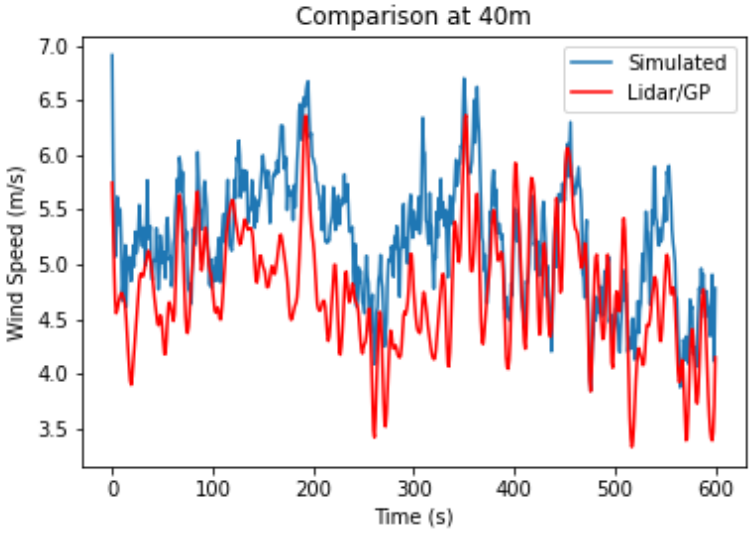

Figure 4.5 Comparison of wind speed outputs from the LiDAR/GP reconstruction at 40m

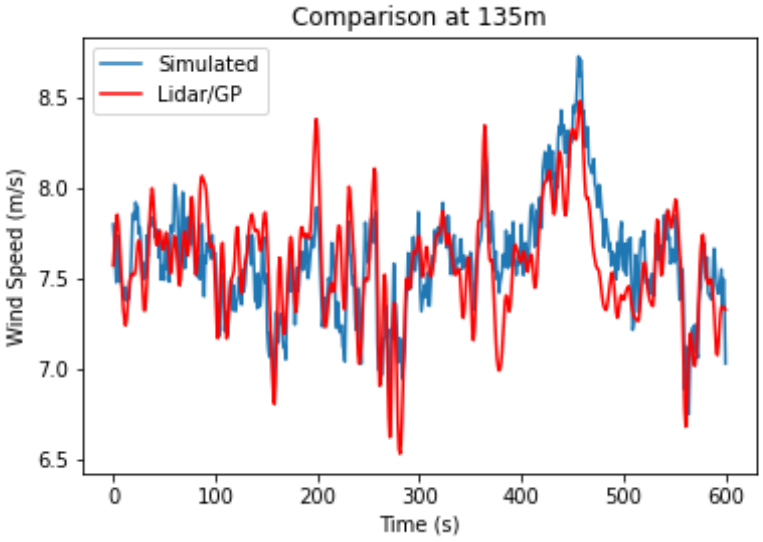

Figure 4.6 Comparison of wind speed outputs from the LiDAR/GP reconstruction at 135m

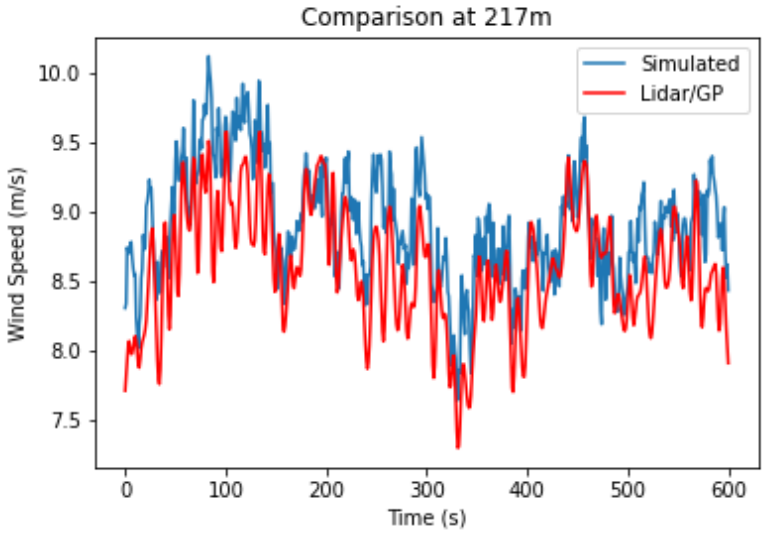

Figure 4.7 Comparison of wind speed outputs from the LiDAR/GP reconstruction at 217m

The difference in overall speed is due to Pyconturb forcing a perfect shear profile when simulating the data, following IEC guidelines. While an option exists to follow the data exactly, this causes irregularities at heights where there is no constraining data. In these regions, Pyconturb will default to a constant profile, keeping the wind speed from the closest measurement. For example, in Figure 4.5, it can be seen that the LiDAR wind speed at 40m is around 4.7 m/s, which would then propagate to all heights below this point. This forcing of a power-law wind profile means that the provided turbulence boxes may miss irregular flow behaviours. Figure 4.8 shows the mean and standard deviations of the longitudinal component of the wind across heights for a different time period, March 20th, 2021 at 19:30. Above hub height, the

wind shows a near-constant profile, and as such the simulated data from Pyconturb is inaccurate here.

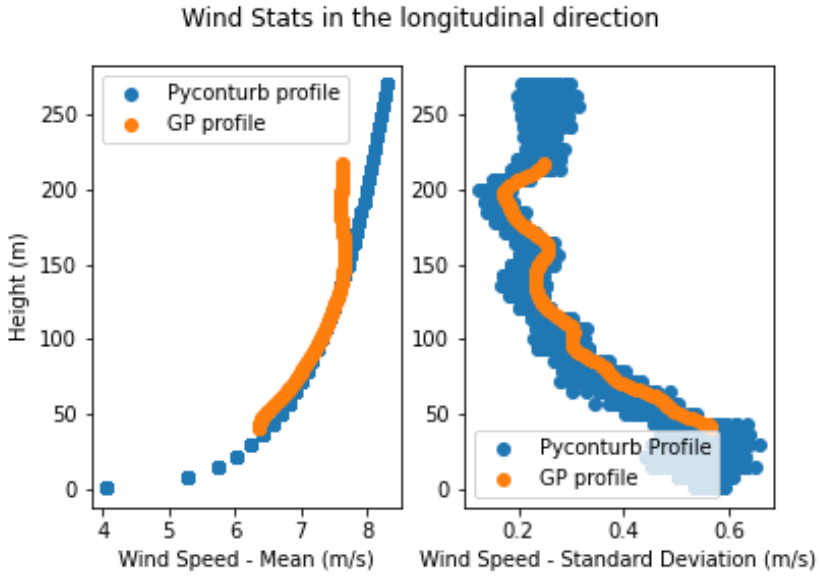

Figure 4.8 Wind speed average (left) and standard deviation (right) for the Pyconturb longitudinal wind speed profile on March 20th, 2021, 19:30. Mean values are included for the LiDAR/GP averages, for comparison

Figure 4.9 and Figure 4.10 show, for the reference time, the lateral and vertical profiles. It can be seen that while a constant zero-mean is enforced in the Pyconturb simulations, this might not align with actual wind conditions. Veer is unable to be handled in current iterations of Pyconturb, and neither are variable vertical wind speeds, leading to differences between the measured data and the provided turbulence boxes.

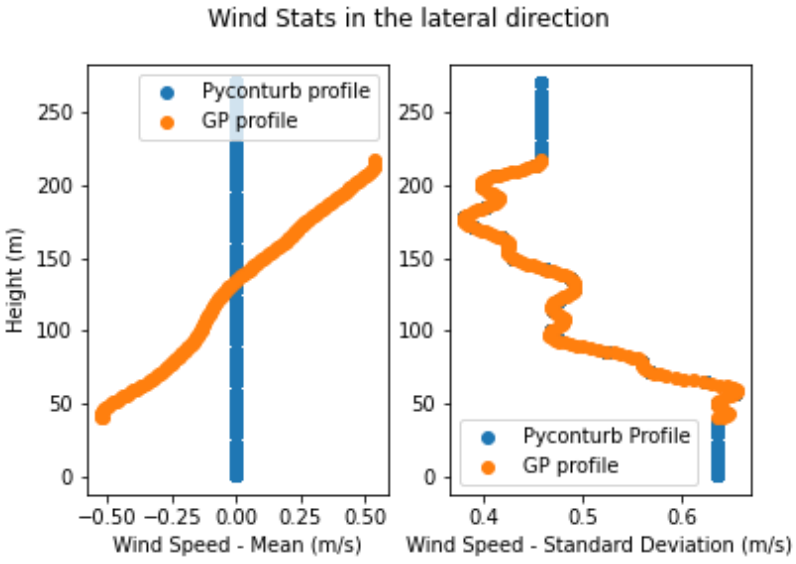

Figure 4.9 Wind speed average (left) and standard deviation (right) for the Pyconturb lateral wind speed profile at the reference time. Mean values are included for the LiDAR/GP averages, for comparison

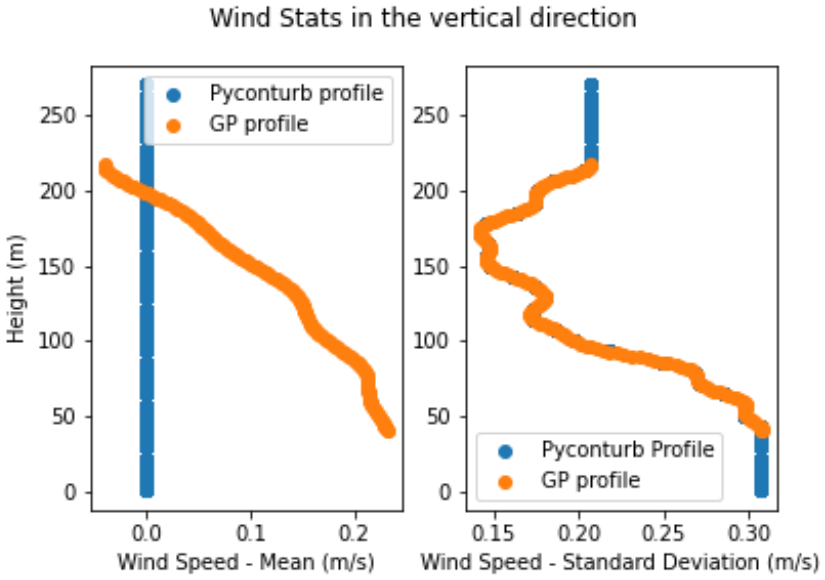

Figure 4.10 Wind speed average (left) and standard deviation (right) for the Pyconturb vertical wind speed profile at the reference time. Mean values are included for the LiDAR/GP averages, for comparison

5 Conclusion

From the results presented in the previous sections, it can be concluded that the Gaussian Process reconstruction methods can be apply to LiDAR measurements to produce high temporal and spatial resolution wind speed prediction for a wind profile. By using the prediction along the LOS's beams, the uncertainty is reduced to the minimum and the GP allows to produce a higher resolution estimation by applying the homogenous reconstruction with prediction at each meter height. This higher resolution of data can be then used as input to Pyconturb to estimate the wind field. The new input data have higher resolution in space and time, compared to the standard 10/12 measurements points provided by the LiDAR.

With respect of the wind field reconstruction methodology based on statistical modelling, the GP's modelling presents a limitation due to its uncertainty where measurements are not available. Nevertheless, the statistical model provides a valid methodology to translate radial wind speed into horizontal wind speed. It has been concluded that significantly improvement can be done by further researching in the estimation of the volume of radial wind speed with a particular focus in the areas with higher uncertainty. This will allow a more accurate estimation and an improvement in the wind field reconstruction based only on GP's and the developed statistical model.

In conclusion, a methodology combining GP's and statistical modelling is developed and described in this report. It is tested with a lower grid resolutions to provide insight in the results. Space for improvement has been highlighted, in particular in regards to the reduction of uncertainty.

6 References

[1] J. Rinker, “PyConTurb,” DTU Wind Energy, 2022. [Online]. Available: https://pyconturb.pages.windenergy.dtu.dk/pyconturb/.

[2] A. Pian and G. Bergman, “TKI WOZ R&D EloQuENT: measurement campaign analysis and time series selection,” TNO R12234, Petten, 2021.

[3] C. Stock-Williams, P. Mazoyer and S. Combrexelle, “Wind field reconstruction from lidar measurements at high-frequency using machine learning,” *Journal of Physics,* p. 1102 012003, 2018.

[4] C. Stock-Williams, G. Bergman and J. Duncan, “Validation at High Frequency of Wind Field Reconstruction from Scanning Lidar using Gaussian Processes,” TNO 2019 R10059, Petten, 2019.

[5] C. Stock-Williams, “Gaussian Process Regression for Wind Field Reconstruction from Lidar,” ECN, Petten, 2017.

[6] C. Stock-Williams, E. Fritz, J. Wagenaar and G. Bergman, “Scanning LiDAR measurements in Rotterdam harbour,” TNO 2019 R11982, Petten, 2019.

[7] G. H. &. P. Ltd, “Bladed User Manual version 4.9,” DNV GL, Bristol, BS2 0PS, UK, 2018.

[8] Leosphere, “WindCube V2 User Manual,” Leosphere, Orsay, 2011.

[9] “RStan,” cran.r-project.org, 18 12 2021. [Online]. Available: https://cran.r-project.org/web/packages/rstan/vignettes/rstan.html.

[10] J. M. Rinker, “PyConTurb: an open-source constrained turbulence generator,” *Journal of Physics: Conference Series,* vol. 1037, no. 6, 2018.

[11] GE, “Haliade X Offshore Turbine,” 2022. [Online]. Available: https://www.ge.com/renewableenergy/wind-energy/offshore-wind/haliade-x-offshore-turbine.

[12] International Electrotechnical Commision, “Wind turbines - part 1: design requirements,” International Electrotechnical Commission, 2005.

[13] A. Sathe, R. Banta, L. Pauscher, K. Vogstad, D. Schlipf and S. Wylie, “Estimating Turbulence Statistics and Parameters from Ground- and Nacelle-Based Lidar Measurements: IEA Wind Expert Report,” DTU Wind Energy, 2015.